

## Index to Supplementary Materials

### **Supplementary Figure 1**

Anti-Trask antibody controls

### **Supplementary Figure 2**

Anti-phospho-Trask antibody controls

### **Supplementary Figure 3**

Effect of delays in fixation on p-Trask staining

### **Supplementary Figure 4**

Effect of depth of fixation on p-Trask staining

### **Supplementary Figure 5**

p-Trask antibody in western blotting

### **Supplementary methods**

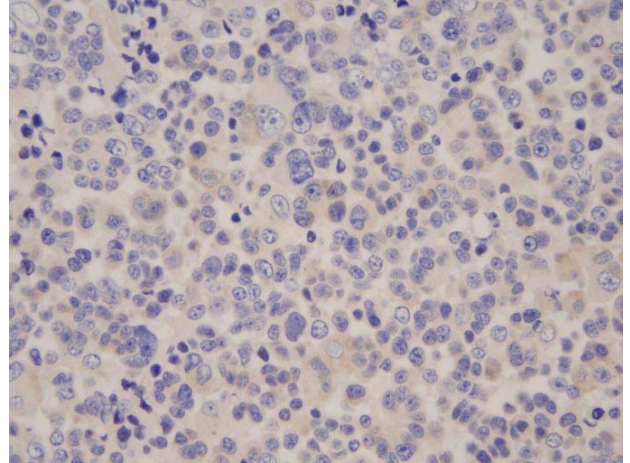
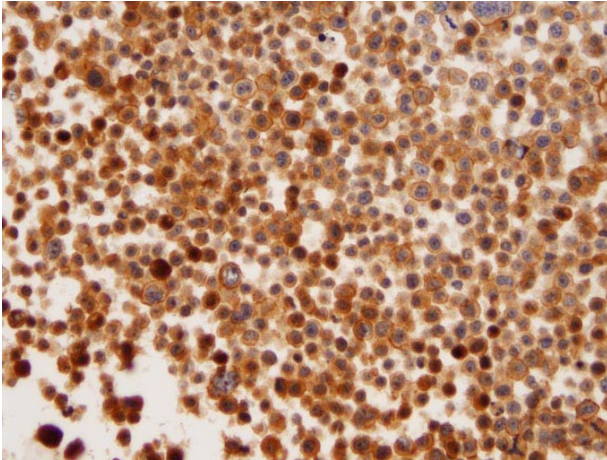
Purification of dasatinib

# Supplementary figure 1

## rabbit anti-Trask antibody controls

MDA-468

MCF7



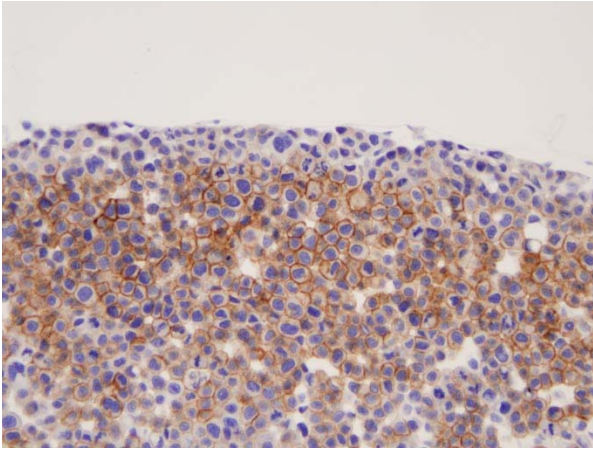
### **Supplementary Figure 1: Controls for anti-Trask rabbit antibody.**

Cultured MDA-468 and MCF-7 cells were scraped and pelleted, fixed in formalin overnight, and embedded in paraffin. 5 micron sections were stained with anti-Trask rabbit antibodies as described in methods. MCF-7 cells have no expression of Trask by western blot or RT-PCR analyses and serve as a negative control. MDA-468 cells have abundant expression of Trask by western blotting and serve as a positive control.

## Supplementary figure 2

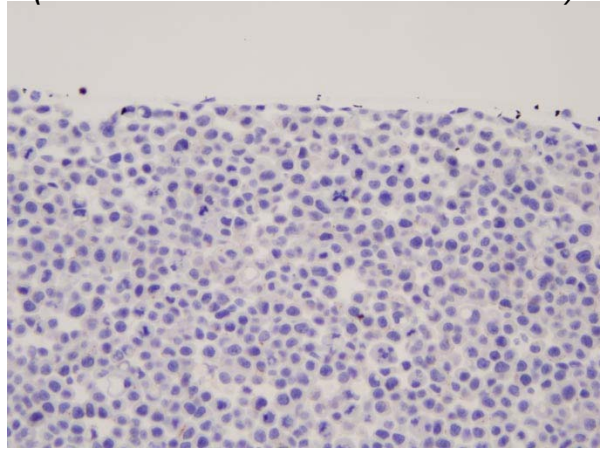
### rabbit anti-phospho-Trask antibody controls

MDA-468

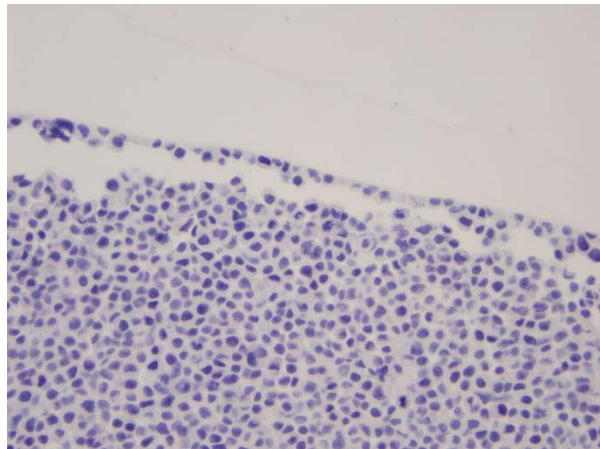


MDA-468

*(treated with dasatinib for 1 hour)*



MCF-7

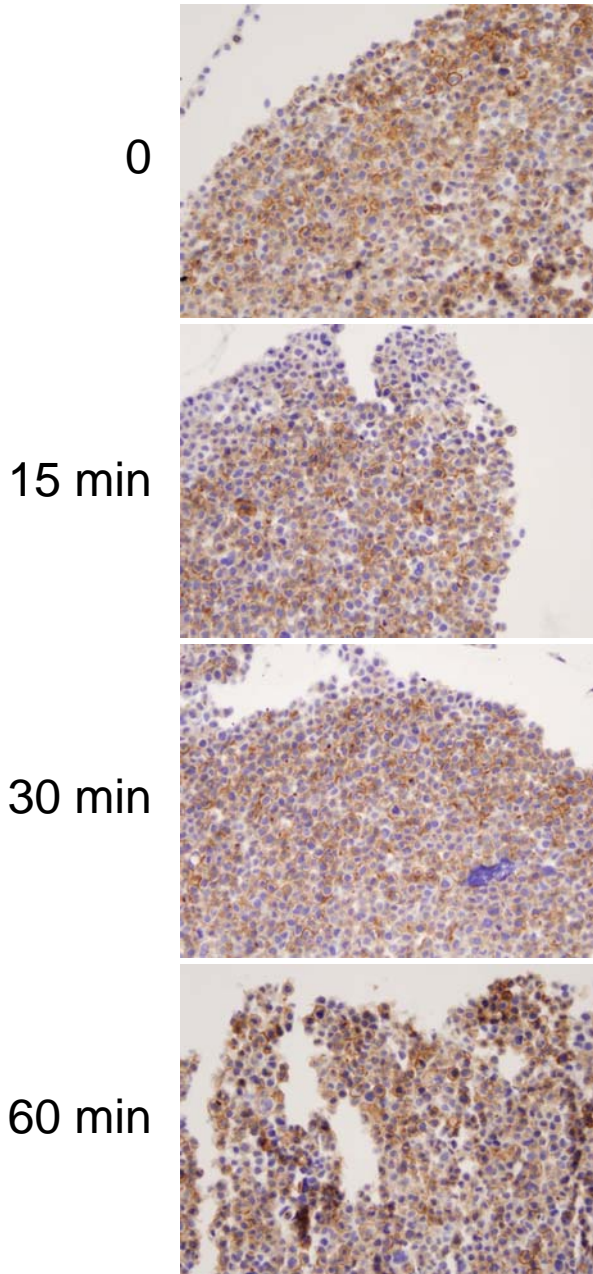


#### **Supplementary Figure 2: Phospho-Trask antibody controls**

Cultured MDA-468 and MCF-7 cells were scraped and pelleted, fixed in formalin overnight, and embedded in paraffin. A separate plate of MDA-468 cells was first treated with 1 μM dasatinib for one hour and subsequently pelleted, fixed, and embedded. 5 micron sections were stained with anti-phospho-Trask rabbit antibodies as described in methods. MCF-7 cells have no expression of Trask by western blot or RT-PCR analyses and serve as a negative control. MDA-468 cells have abundant expression and phosphorylation of Trask by western blotting and serve as a positive control. Dasatinib-treated MDA-468 cells have complete dephosphorylation of Trask by phosphotyrosine immunoblots of anti-Trask immunoprecipitates and serve as another negative control.

# Supplementary figure 3

## Effects of delays in fixation:



### **Supplemental Figure 3:**

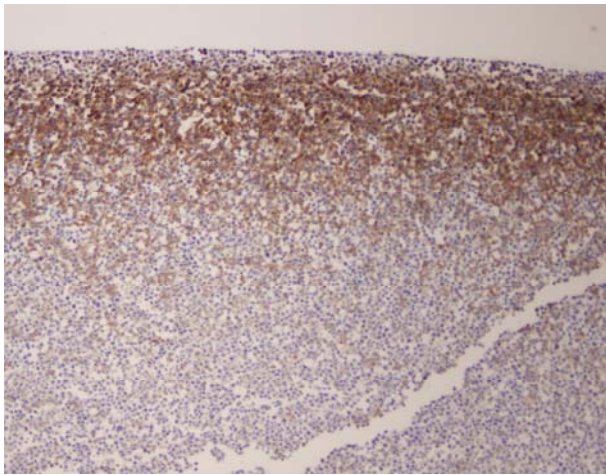
#### **Estimating phospho-Trask decay due to delays in fixation**

Since the analysis of surgical specimens using phospho-specific antibodies is often compromised by variable lengths of delays that are incurred from the time of resection to the time of fixation, we studied the effect of delayed fixation on preservation of Trask phosphorylation in our positive control cell line model. MDA-468 cells were scraped and pelleted. At that point, they were either placed immediately in formalin (0 timepoint), or left on the bench for the indicated amounts of time and subsequently placed in formalin. After overnight fixation, pellets were embedded in paraffin, and 5 micron sections stained with anti-phospho-Trask antibodies as described in methods. Although the quality of the tissue begins to decline with decays of an hour, the phosphorylation of Trask does not decay rapidly and is still present even with an hour in delay time. The previously shown negative controls were included in this analysis.

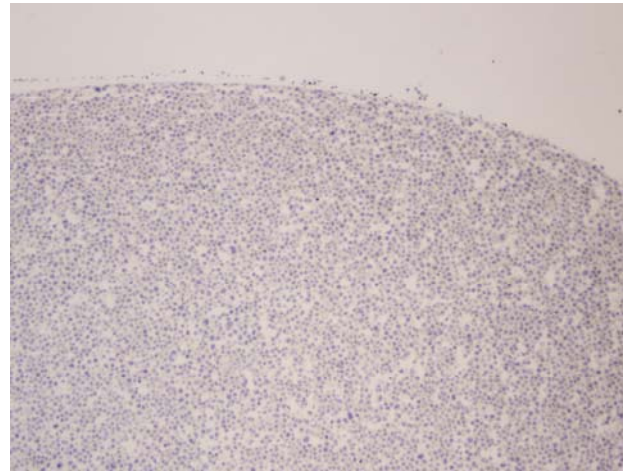
## Supplementary figure 4

Effects of depth of fixation:

**MDA-468**



**MDA-468 +  
src inhibitor**

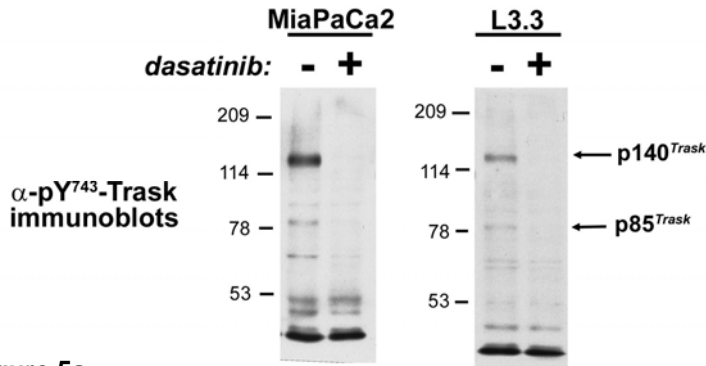


### **Supplementary Figure 4: The effects of depth of fixation on p-Trask preservation**

Since the immunohistochemical analysis of phospho-proteins from surgical specimens is known to be complicated by numerous artifactual variables, we also examined the effect of depth of tissue fixation on phospho-Trask signal preservation. Looking at formalin-fixed paraffin embedded pellets from our positive control MDA-468 cells, we observed that phospho-Trask staining was only evident in the outer 1-2mm of the pellet. This staining is a true positive staining since it is not seen in a negative control prepared side-by-side with this specimen. The negative control is the src inhibitor treated MDA-468 cell pellet. This phenomenon is reproducible and identical findings were seen with several preparations of cell pellets over time and also seen in our examination of the archival human tissue material. It is well known that formalin penetrates tissues slowly, and certain epitopes within deeper sections are not preserved or fixed well enough. Therefore in our analysis of human tissues and tumors from surgical specimens, we focused on the outer areas of the tissue blocks for reliable phospho-Trask staining data.

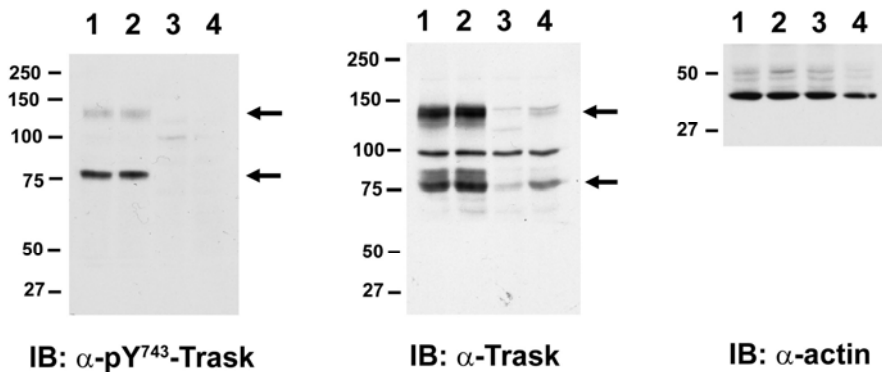
# Supplementary figure 5

## Specificity of the anti-phospho-Trask antibody



### Supplemental Figure 5a:

MiaPaCa2 and L3.3 pancreatic cancer cells were treated with 1uM dasatinib or DMSO for 1 hour. Total cell lysates were immunoblotted using the indicated antibodies. As seen here, Trask is rapidly dephosphorylated by treatment with dasatinib. Similar results are seen with other src inhibitors including PP1 (not shown).



### Supplemental Figure 5b:

Cell lysates from MDA-468 cells and its anti-Trask shRNA transfectants were immunoblotted with the indicated antibodies. Lanes correspond to: 1) untransfected MDA-468 cells, 2) MDA-468 cells transfected with a non-silencing shRNA control, 3,4) MDA-468 cells transfected with two different anti-Trask shRNA sequences.

These data show the specificity of the anti-pY743-Trask antibody for Trask (figure 5b) and for the phosphorylated form of Trask (figure 5a).

## Supplemental methods

### Purification of dasatinib

Solvents, of the highest grade, were all obtained from Aldrich. Also, we recorded the  $^1\text{H}$  NMR spectrum at 400 MHz on a Varian Innova 400 spectrometer. With a mortar and pestle, we pulverized ten Sprycel tablets (Bristol-Myers Squibb, 70 mg dose, "524" marking) and transferred the resulting powder to an Erlenmeyer flask. We added 20 mL DMF to the flask, sonicated the suspension for 30 min at rt and passed the resulting slurry through a pad of Celite, which we washed with 25 mL DMF. Concentration of the filtrate under vacuum gave a white powder, which we dissolved in 25 mL 14.5 : 10.5 : 2.5 MeOH : EtOAc : 2 M aq.  $\text{NH}_4\text{OH}$ . We sonicated this suspension at rt for 30 min and removed the insoluble material by filtering the slurry through a pad of Celite that was then rinsed with an additional 25 mL 14.5 : 10.5 : 2.5 MeOH : EtOAc : 2 M aq.  $\text{NH}_4\text{OH}$ . We obtained a white powder by concentrating the filtrate under vacuum in a round bottom flask. Recrystallization of the crude product from approximately 5 mL 80 % (v/v) EtOH in  $\text{dH}_2\text{O}$  with heating from a heat-gun gave a clear, pale yellow solution. We transferred the solution to an 18 × 150 mm glass culture tube and allowed the solution to cool. While the glass tube was warm to the touch, we added rt  $\text{dH}_2\text{O}$  dropwise until the solution just turned cloudy. Shiny white crystals formed within 30 min. Using Buchner vacuum filtration, we collected the crystals and rinsed them with several portions of  $\text{dH}_2\text{O}$  to afford a white powder. We purified 30 Sprycel tablets using this procedure, averaging 40 % by weight recovery of the dasatinib amount listed on the Sprycel packaging. The proton NMR data of the recovered crystals matched the patent literature values<sup>1</sup> for the monohydrate form of dasatinib:  $^1\text{H}$  NMR ( $\text{DMSO}-d_6$ )  $\delta$  11.45 (s, 1H), 9.86 (s, 1H), 8.21 (s, 1H), 7.40 (dd,  $J=7.3, 1.5$  Hz, 1H), 7.29 (m, 1H), 7.25 (app. t, 1H), 6.05 (s, 1H), 4.43 (t,  $J=5.3$  Hz, 1H), 3.56–3.47 (m, 6H), 2.47 (m, 4H), 2.45–2.38 (m, 5H), 2.24 (s, 3H).

<sup>1</sup> Chen, B.-C.; Droghini, R.; Lajeunesse, J.; Dimarco, J. D.; Galella, M.; Chidambaram, R. Preparation of 2-aminothiazole-5-aromatic carboxamides as kinase inhibitors. WO 2005077945, February 4, 2005.